

Letters to ESEX

High resolution transmission electron microscopy evaluation of silica glaze reveals new textures

K. A. Langworthy,¹ D. H. Krinsley² and R. I. Dorn^{3*}

¹ CAMCOR, University of Oregon, Eugene, OR, USA

² Department of Geological Sciences, University of Oregon, Eugene, OR, USA

³ School of Geographical Sciences and Urban Planning, Arizona State University, Tempe, AZ, USA

Received 9 March 2010; Revised 14 June 2010; Accepted 15 June 2010

*Correspondence to: R. I. Dorn, School of Geographical Sciences and Urban Planning, Arizona State University, Tempe, AZ 85287-5302, USA.
E-mail: ronald.dorn@asu.edu

ESPL

Earth Surface Processes and Landforms

ABSTRACT: We present the first nanoscale investigation of silica glaze. High resolution transmission electron microscopy of a rock coating from the Ashikule Basin, Tibetan Plateau, reveals the presence of spheroids composed predominantly of silicon and oxygen with diameters ranging from 20 nm to 70 nm. While silica glaze spheroids co-exist with manganese-rich rock varnish in the same sample, the different rock coatings are texturally and physically distinct at the nanoscale. These observations are consistent with a model of silica glaze formation starting with soluble aluminum-silicon (Al-Si) complexes $[\text{Al}(\text{OSi}(\text{OH})_3)_2]^{2+}$, mobilized with gentle wetting events such as dew or frost. The transition between complete and partial wetting on silica surfaces rests at about 20–70 nm for liquid droplets. Upon crossing this transition, a metastable wetting film would be ruptured, initiating formation of silica glaze through spheroid deposition. Copyright © 2010 John Wiley & Sons, Ltd.

KEYWORDS: focused ion beam; HRTEM; rock coatings; silica glaze; Tibet; weathering

Introduction

Rock coatings of mostly silica, or silica glaze (Butzer *et al.*, 1979; Smith, 1988; Dorn, 1998), can be found in virtually every terrestrial environment. In warm deserts 'thin, colorless, transparent, highly lustrous coatings' (Fisk, 1971) have been noted in Egypt (Hobbs, 1918), in south-eastern Libya (Haberland, 1975), on gibbers (Jessup, 1960) and bedrock faces in Australia (Watchman, 1992), throughout the western United States drylands (Stevenson, 1881; Perry *et al.*, 2006), in the Gobi (Zhu *et al.*, 1985) and other warm deserts (Dorn, 2009). Silica-dominant coatings with different hues and chromas are also found on bedrock in front of glaciers (Whalley *et al.*, 1990), under glaciers (Peterson and Moresby, 1979), in the rainshadow of warm arid islands like Hawaii and Vulcano (Curtiss *et al.*, 1985; Minitti *et al.*, 2007; Chemtob *et al.*, 2010), on temperate subaerial surfaces (Robinson and Williams, 1987), on Antarctic rocks (Weed and Ackert, 1986), coating joint faces (Robinson and Williams, 1992), in fault zones (Schindler *et al.*, 2010), and coating alluvial boulders along tropical rivers (Alexandre and Lequarre, 1978).

The importance of silica glaze rests in several areas of earth surface processes. It is a dominant rock coating in many terrestrial weathering environments, and understanding its genesis may provide clues in interpreting landscape geochemical shifts in environmental conditions (Perel'man, 1966; Fortescue, 1980). Silica glaze can mobilize and reprecipitate inside the

weathering rind of rocks; this process helps case harden rock surfaces (Conca and Rossman, 1982; Conca and Astor, 1987; Weed and Norton, 1991; Young and Young, 1992). Silica glaze covers buildings in polluted urban settings (McAlister *et al.*, 2006; Smith *et al.*, 2007), rock paintings (Watchman, 1985), rock engravings (Tratebas *et al.*, 2004), and stone monuments (Paradise, 2005) and can act as an agent of rock art stability (Dorn *et al.*, 2008). There are also suggestions that silica glaze may be present as a rock coating on Mars (Dorn, 1998; Kraft and Greeley, 2000; Kraft *et al.*, 2004; Perry and Lynne, 2006).

Wavelength dispersive electron microprobe analyses of silica glaze reveals six general types (Dorn, 1998):

Type 1: a largely homogenous amorphous silica glaze.

Type 2: abundance of detrital grains cemented by amorphous silica.

Type 3: aluminum and iron are major components along with silica.

Type 4: aluminum is a major component along with silica.

Type 5: iron is a major component along with silica.

Type 6: the abundance of amorphous silica is less than aluminum.

Investigations of *in situ* weathering of plagioclase reveal that Type 1 silica glazes can substantially reduce dissolution rates, compared to adjacent uncoated plagioclase minerals (Gordon and Dorn, 2005b). Light and low-resolution electron microscopy, however, does not allow for easy identification of these categories in a sample.

A major difficulty conducting research on the origin of silica glaze and its potential paleoenvironmental significance is the difficulty of linking silica glaze composition and the environment of formation through secondary electron (SE) and back-scattered electron (BSE) imagery; results have shown mostly homogenous textures (Figure 1a), with the exception of the presence of detrital grains (Figure 1b). This appears to be the case even when silica glaze interdigitates with other rock coatings (Dorn, 1998). Thus, this paper explores the use of high resolution transmission electron microscopy (HRTEM). This approach takes advantage of using a dual beam – focused ion beam (DB-FIB) (Uchic *et al.*, 2007) to prepare samples for analysis at resolutions of about 0.8 Å.

Study Site

The sample of silica glaze in our study comes from the Ashikule Basin on the Tibet Plateau, located on the north side of the west Kunlun Mountains (Figure 2). Collected from a late Pleistocene trachyandesite lava flow of the Ashishan Volcano (Wei *et al.*, 2003), the specific outcrop had experienced wind abrasion in the past as evidenced by a grooved and polished ventifacted surface. Aeolian abrasion, however, ceased at some point to permit the formation of rock coatings that would have been otherwise eroded. The sample was collected between 4700 and 4800 m in elevation. Two nearby playas, Ashikule and Urukele, deflate carbonate and sulfate mineral dust in the Ashikule Basin. We selected this locale for study in part because the environment is both arid and cold (Wu and Qian, 2003), with both dew and frost (Goldstein and Beall, 1990). Hence, the findings could have potential relevance for research in both arid and alpine weathering settings.

Silica glaze is not the only rock coating present, as is often the case in terrestrial weathering environments. Several different types of rock coatings are found at this study site (see chapter 15 in Dorn, 1998). Gypsum and carbonate forms on fracture sidewalls. Oxalates accrete on subaerial surfaces and in fractures. Rock varnish also grows subaerially and in fractures. However, silica glaze is the most common rock coating seen on the lava flow surfaces. The particular sample was selected for DB-FIB preparation and HRTEM analysis, because it displays an interdigitation of rock varnish and silica glaze (Figure 3). As is the case in other samples, the silica glaze appears texturally homogenous in SE and BSE (Figure 3).

Methods

Samples of silica glaze were prepared by cutting a rock chip from a bulk sample, placing the chip in a one-inch lexan ring, then backfilling the ring with liquid epoxy to prevent the sample from crumbling. The plug, with the contained sample, was then ground flat and polished until it was highly reflective. It was then examined and photographed with a reflected light microscope in order to locate areas of interest. After light microscopy, the plug was examined in both BSE and SE modes, using a FEI Helios DB-FIB microscope. Backscatter imaging was used to locate regions of initial interest by utilizing atomic number contrast exhibited by variability in geological minerals.

After locating specific regions of interest, the DB-FIB was used to mill a thin lamella for cross-section analysis in a FEI Titan HRTEM. The lamella was lifted out of the bulk specimen *in situ* with the use of an Omniprobe micromanipulator and attached to a copper transmission electron microscope (TEM) grid through platinum gas ionization/deposition. The section

was further thinned and ion polished with a 20 pA ion beam to produce an approximately 100 nm thick specimen for HRTEM analysis.

During TEM analysis, high kilovolt beam damage was noted when using the spot mode to perform Energy dispersive X-ray spectroscopy (EDS), resulting in low X-ray counts during penetration due to a lack of X-rays in the penetration area. The use of scanning transmission electron microscopy (STEM) mode in the FEI Titan provided extremely good contrast in comparison to bright field TEM, which was useful for phase/grain identification.

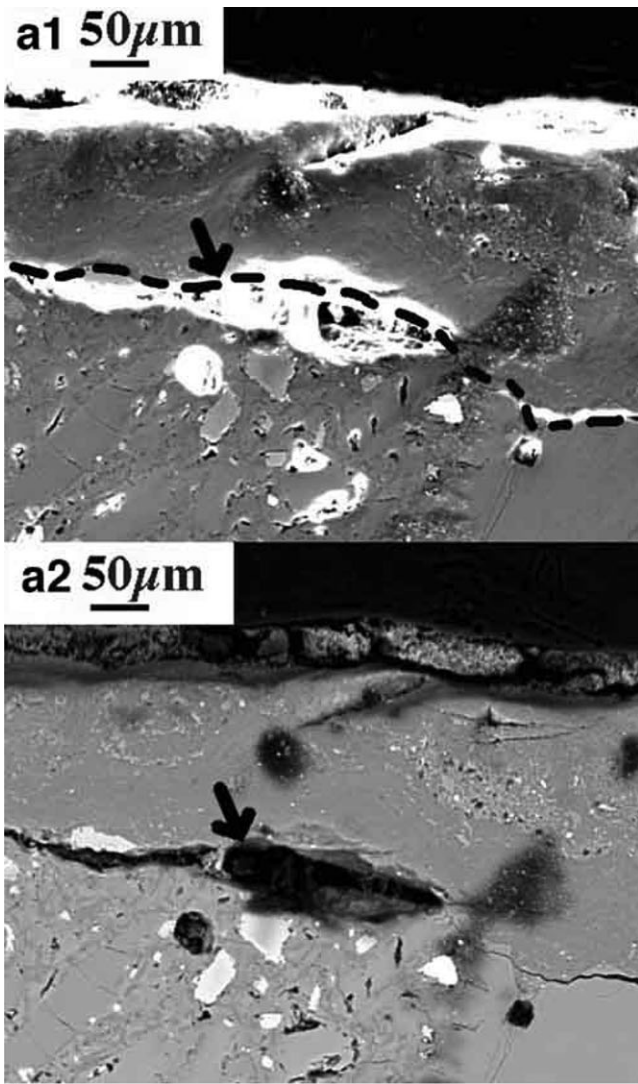
Results and Discussion

The primary finding of this application of DB-FIB sample preparation and HRTEM analysis of rock coatings is that the Tibetan Plateau silica glaze appears to be precipitating in the form of spheroids (Figure 4) with typical diameters of approximately 50 nm (Figure 5). EDS analyses reveal that the spheroids appear to be composed of primarily silicon and oxygen (Figure 4), consistent with prior electron microprobe analyses of silica glazes from the Tibetan Plateau (Dorn, 1998). However, prior analyses were at a scale of a few microns, not nanometers as in this study.

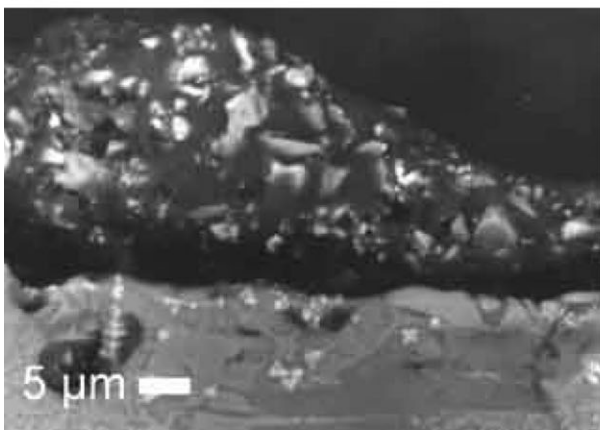
Our observations offer support for a conceptual model of silica glaze formation proposed earlier (Dorn, 1998, chapter 13), with the clear caveat that this nanoscale investigation is for a single sample only. The HRTEM evidence is consistent with a genesis starting with the soluble aluminum-silicon (Al-Si) complexes $[Al(OSi(OH)_3)_2]^{2+}$ that are ubiquitous and are known to play an important role in the formation of metastable minerals at the water–rock interface (Lou and Huang, 1988; Browne and Driscoll, 1992). Even very small and gentle wetting (e.g. dew or frost deposition) would be enough to mobilize these Al-Si complexes. Of particular importance might be a transition between complete and partial wetting on silica surfaces; the transition for nanoscale droplets rests at about 20–70 nm (Zorin *et al.*, 1992; Churaev, 2003) – the same general size range as the observed spheroids. When this transition is crossed, the metastable wetting film on the silica surface is then ruptured (Zorin *et al.*, 1992) and the spheroids would form. The general notion that silicic acid surfaces are not molecularly smooth and can expand or collapse by changes in solutions (Israelachvili and Wennerström, 1996) would be consistent with the appearance of the silica glaze spheroids.

Silica glaze spheroids are most noticeable where there is abundant porosity in the rock coating (Figure 5), allowing growth into space that was formerly a void. Contacts between spheroids appear indistinct, as though spheroid surfaces fused together at some point. The development of nanometer spheroids into voids is consistent with the transition between complete and partial wetting, where droplets ‘do not cling to a surface immediately after formation, but move somewhat before they attach to the [pre-existing] solid’ (Koopal *et al.*, 1999, p. 24).

There are places where the pores appear to have been filled in with additional silica glaze (Figure 6). Filling in pore spaces with silica glaze explains both the relatively homogeneous appearance in BSE and SE imagery and the occurrence of micron-scale voids. Figures 2 and 3, as well as in many other images of silica glaze at this scale (see chapter 13 in Dorn, 1998), display micron-scale voids. We speculate, based on our observations of this single sample, that the spheroids create a lattice structure which is then gradually filled in over time. The transition between spheroids and denser silica glaze where the void spaces are filled in (Figure 6) could relate to the ability of



(a)



(b)

Figure 1. SE and BSE microscopy reveals mostly homogenous textures for silica glazes. (a) Typical homogenous texture, seen here in SE (a1) and BSE (a2) in a sample from a late glacial maximum morainal boulder, Ixtaccihuatl volcano, Mexico. The arrow points to organic matter trapped under the silica glaze. The dashed line in a1 indicates the base of the silica glaze. As in many other BSE and SE images, there are hints of laminations and bits of detritus. However, the overall appearance is relatively homogeneous. [The dark smudge on the right side of the imagery is likely an artifact of sample handling at Arizona State University.] (b) A mostly amorphous texture for the silica glaze even though detrital grains of glass and basalt minerals are incorporated. The sample was collected from the 1859 Mauna Kea lava flow about 5 km east of the western coastline of Hawaii.

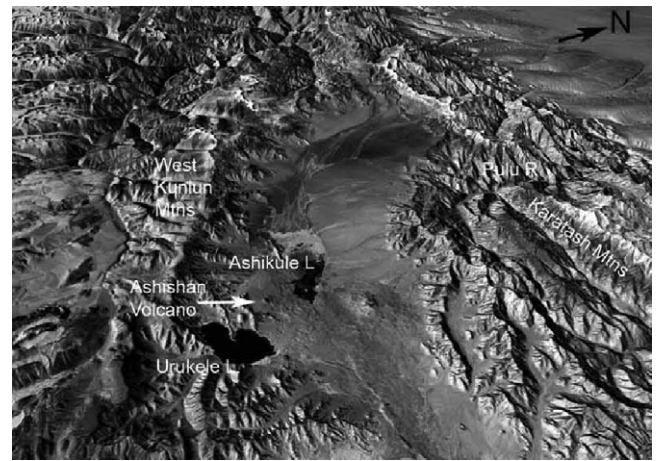


Figure 2. Ashishan Volcano study site in the Ashikule Basin, Tibet at N 35° 41' 55.86" 81° 34' 34.43". The width of the graben at the location of the Ashishan Volcano is about 22 km. The image is courtesy of William Bowen.

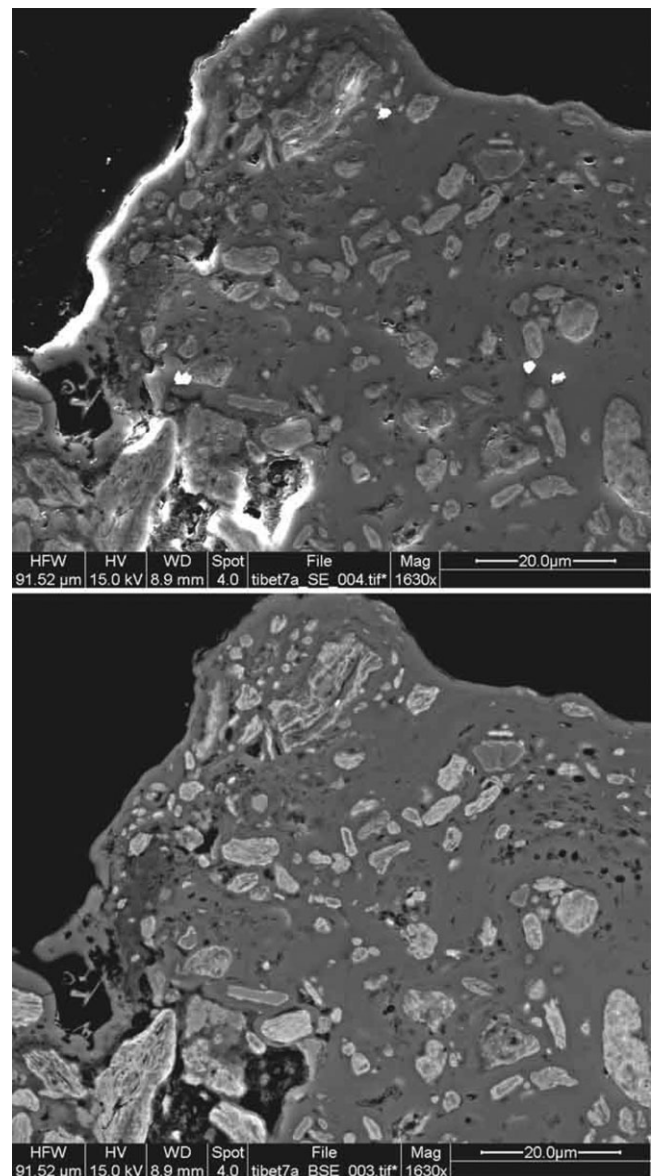


Figure 3. SE (upper) and BSE (lower) images of the sample examined here from the Ashishan Volcano, Tibetan Plateau. The bright "pods" in the BSE image are rock varnish (Krinsley *et al.*, 2009), and these varnish pods contrast with the rock coating that envelopes rock varnish: silica glaze with a homogenous texture.

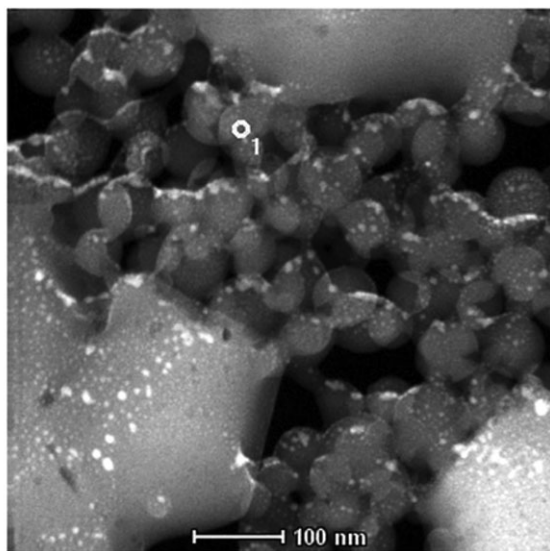
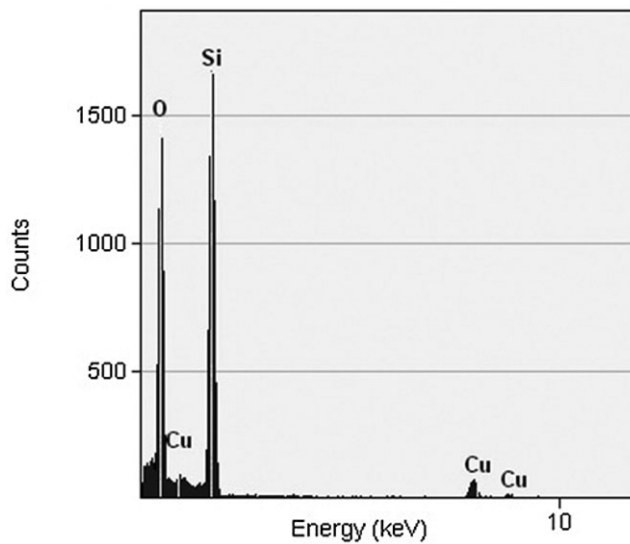


Figure 4. Energy-dispersive X-ray analysis of a spheroid, where the circle and number 1 annotation indicate the approximate location of the analysis. The spheroids consist of silicon and oxygen, while the copper signal is an artifact of the grid holding the sample.

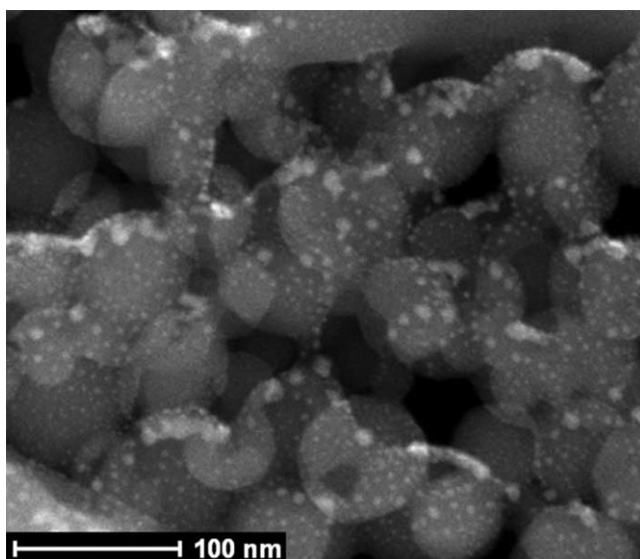


Figure 5. The silica glaze spheroids with abundant porosity. The upper left spheroid is the location of the EDS measurement in Figure 4. The bright dots are artifacts and do not indicate compositional variability in the spheroids.

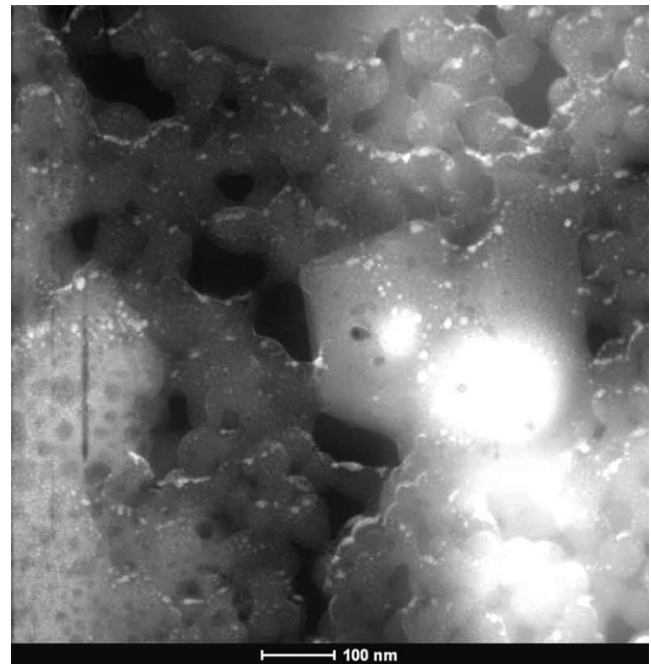


Figure 6. Spheroids where the pore spaces have begun to fill in with additional silica (on the right). Note the semi hexagonal silicon-oxygen-containing object (bright, center-right) that is on top of the spheroids. The spheroids at least partially pass under the object, suggesting that this object may be additional evidence of solution, transport via water and deposition of silica. The bright dots are artifacts and do not indicate compositional variability in the spheroids. The Swiss cheese appearance in the lower left likely represents holes in the thinned specimen and hence is an artifact and not a true texture.

silicic acid and soluble Al-Si complexes to more readily bond to the silica glaze than the rock. 'Silicon need have no residence time in solution as silicic acid before it is incorporated into a solid reaction product at the surface of a mineral' (Casey *et al.*, 1993, p. 255). Thus, the slight tendency for layering sometimes seen in BSE at the micron scale could be this later stage of filling in the voids.

Curtiss *et al.* (1985) recognized the silica glaze on Hawaiian lava flows was not stable and could form and erode on decadal timescales. Other work on silica glazes indicates both physical and chemical instability, where silica glaze can remobilize and impregnate the underlying pore spaces in the host rock (Tratebas *et al.*, 2004; Gordon and Dorn, 2005a, 2005b; Krinsley *et al.*, 2009). Other evidence of the instability of silica glaze comes from radiocarbon dating of organic matter at the interface of silica glaze and the underlying late glacial maximum morainal boulder from Ixtaccíhuatl volcano, Mexico (Figure 1a). The carbon-14 (^{14}C) age of 2870 ± 50 (Beta 99293) reported by Dorn (1998) is far younger than the late-Pleistocene age of the moraine – providing additional evidence for geochemical instability of silica glaze over millennial timescales. The imagery presented here (e.g. Figure 6) could explain the aforementioned observations that silica glazes are physically and chemically unstable. Our initial interpretation of HRTEM imagery from this one site is that pore spaces between spheroids gradually infill, solidifying and stabilizing silica glaze. However, this infilling process need not occur. We speculate that silica glaze instability (Curtiss *et al.*, 1985; McAlister *et al.*, 2006; Smith *et al.*, 2007) could be associated with those intra-glaze locations with an abundance of inter-spheroid porosity.

Just as silica glaze interdigitates with varnish at the micrometers scale (Figure 3), silica glaze spheroids similarly

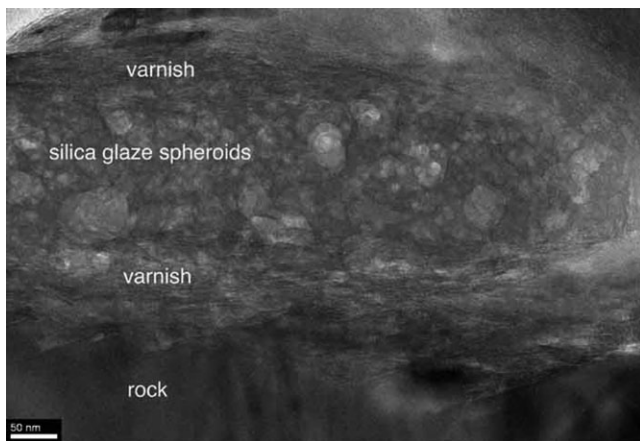


Figure 7. Silica glaze interdigitates with rock varnish, even at the nanometer scale. Here, layered varnish rests on top of and underneath silica glaze composed of spheroids. The dark tone at the bottom is a rock mineral. Note how the varnish rests distinctly on the underlying rock and how the silica glaze spheroids in turn makes a distinct contact with the varnish. EDS analysis of the middle zone reveals that the spheroids are composed of silicon and oxygen, similar to Figure 4.

appear to interdigitate with rock varnish at the nanometer scale (Figure 7). The reason for a sudden switch in the type of rock coating that forms from varnish to silica glaze could relate to environmental change associated with the chemistry and abundance of dust fallout. A higher pH, as a result of alkali-rich aeolian fines mixing with melting snow, would generate higher concentrations of silica; silicon is more mobile at higher pH values in terrestrial weathering settings (NIAIST, 2005) and thus could be at higher concentrations in droplets. A second possible explanation for a nanoscale switch between varnish and silica glaze could be produced by a paucity of manganese and iron to cement clays and form rock varnish or iron films. This is because higher pH values result in the oxidized manganese and iron that is immobile in water (NIAIST, 2005). Both abiotic and biotic explanations for manganese and iron enhancement in rock varnish require that manganese and iron be available in the divalent mobile state (Dorn, 1998).

A notion in the literature that silica glaze and rock varnish are somehow part of the same general depositional process (Perry and Lynne, 2006; Perry and Sephton, 2007) has been disputed (Dorn, 2007). Micron scale imagery showed that these rock coatings are morphologically distinct (Dorn, 2009; Krinsley *et al.*, 2009). HRTEM imagery (Figure 7) also shows that these two rock coatings are quite distinct, even at nanometer scales.

Conclusion

Silica glazes are one of the most common rock coatings found at the Earth's surface, occurring in all terrestrial weathering environments – from the cold-dry deserts of Antarctica to the humid tropics. Previous studies, limited to the micrometer scale, have generated imagery showing very little textural differentiation. Our nanoscale study using HRTEM analysis, and in particular STEM mode, reveals that silica glazes are not as homogeneous as previous SE and BSE imagery would suggest. A sample of silica glaze from the Ashikule Basin of the Tibetan Plateau contains 20 to 70 nm diameter spheroids composed predominantly of silicon and oxygen. Although manganese-bearing rock varnish interdigitates in the same sample, it is texturally

quite distinct and shows no evidence of subtle nanoscale facies changes between silica glaze and varnish.

Although this first nanoscale study was carried out on just one sample, our observations are consistent with silica glaze starting as soluble Al-Si complexes $[Al(OSi(OH)_3)_2]^{2+}$ in gentle wetting events such as dew or frost. Since the transition between complete and partial wetting on silica surfaces rests at about 20–70 nm, the same size range as the observed spheroids, crossing this transition would rupture a metastable wetting film, forming the spheroids and starting the process of silica glaze formation. Future nanoscale investigations of other samples would provide tests of our proposed hypothesis for silica glaze genesis.

Acknowledgments—The authors thank Dr Tanzhuo Liu for collection of the sample, Dr Sujing Xie for assistance on the HRTEM, and the suggestions of anonymous reviewers.

References

- Alexandre J, Lequarre A. 1978. Essai de datation des formes d'érosion dans les chutes et les rapides du Shaba. *Geo-Eco-Trop* **2**: 279–286.
- Browne BA, Driscoll CT. 1992. Soluble aluminum silicates: stoichiometry, stability, and implications for environmental geochemistry. *Science* **256**: 1667–1669.
- Butzer KW, Fock GJ, Scott L, Stuckenrath R. 1979. Dating and context of rock engravings in South Africa. *Science* **203**: 1201–1214.
- Casey WH, Westrich HR, Banfield JF, Ferruzzi G, Arnold GW. 1993. Leaching and reconstruction at the surfaces of dissolving chain-silicate minerals. *Nature* **366**: 253–256.
- Chemtob SM, Jolliff BL, Rossman GR, Eiler JM, Arvidson RE. 2010. Silica coatings in the Ka'u Desert, Hawaii, a Mars analog terrain: a micromorphological, spectral, chemical and isotopic study. *Journal of Geophysical Research* **115**: E04001. DOI: 10.1029/2009JE003473
- Churaev NV. 2003. Surface forces in wetting films. *Advances in Colloid and Interface Science* **103**: 197–218.
- Conca JL, Rossman GR. 1982. Case hardening of sandstone. *Geology* **10**: 520–525.
- Conca JL, Astor AM. 1987. Capillary moisture flow and the origin of cavernous weathering in dolerites of Bull Pass Antarctica. *Geology* **15**: 151–154.
- Curtiss B, Adams JB, Ghiorso MS. 1985. Origin, development and chemistry of silica-alumina rock coatings from the semiarid regions of the island of Hawaii. *Geochemica et Cosmochimica Acta* **49**: 49–56.
- Dorn RI. 1998. *Rock Coatings*. Elsevier: Amsterdam.
- Dorn RI. 2007. Baking black opal in the desert sun: the importance of silica in desert varnish. Comment. *Geology* v. DOI: 10.1130/G23410C.1
- Dorn RI. 2009. Desert rock coatings. In *Geomorphology of Desert Environments*, Parsons AJ, Abrahams A (eds). Springer: Amsterdam; 153–186.
- Dorn RI, Whitley DS, Cerveny NC, Gordon SJ, Allen C, Gutbrod E. 2008. The rock art stability index: a new strategy for maximizing the sustainability of rock art as a heritage resource. *Heritage Management* **1**: 35–70.
- Fisk EP. 1971. Desert glaze. *Journal Sedimentary Petrology* **41**: 1136–1137.
- Fortescue JAC. 1980. *Environmental geochemistry. A holistic approach*. Springer-Verlag: New York.
- Goldstein MC, Beall CM. 1990. *Nomads of Western Tibet*. University of California: Berkeley, CA.
- Gordon SJ, Dorn RI. 2005a. In situ weathering rind erosion. *Geomorphology* **67**: 97–113.
- Gordon SJ, Dorn RI. 2005b. Localized weathering: implications for theoretical and applied studies. *Professional Geographer* **57**: 28–43.
- Haberland W. 1975. Untersuchungen an Krusten, Wustenlacken und Polituren auf Gesteinsoberflächen der nördlichen und mittleren

- Saharan (Libyen und T Chad) [Investigation of weathering rinds, coatings, and polishes in the typical lichen upland of the northern Saharan]. *Berliner Geographische Abhandlungen* **21**: 1–77.
- Hobbs WH. 1918. The peculiar weathering processes of desert regions with illustrations from Egypt and the Soudan. *Michigan Academy of Sciences Annual Report* **20**: 93–98.
- Israelachvili J, Wennerström H. 1996. Role of hydration and water structure in biological and colloidal interactions. *Nature* **379**: 219–225.
- Jessup RW. 1960. The stony tableland soils of the southeastern portion of the Australian arid zone and their evolutionary history. *Journal Soil Science* **11**: 188–196.
- Koopal LK, Goloub T, de Keizer A, Sidorova MP. 1999. The effect of cationic surfactants on wetting, colloid stability and flotation of silica. *Colloids and Surfaces A: Physicochemical and Engineering Aspects* **151**: 15–25.
- Kraft MD, Greeley R. 2000. Rock coatings and aeolian abrasion on Mars: application to the Pathfinder landing site. *Journal of Geophysical Research – Planets* **105**(E6): 15107–15116.
- Kraft MD, Michalski JR, Sharp TG. 2004. High-silica rock coatings: TES surface-type 2 and chemical weathering on Mars. *Lunar and Planetary Science* **35**: 1936.
- Krinsley D, Dorn RI, DiGregorio BE. 2009. Astrobiological implications of rock varnish in Tibet. *Astrobiology* **9**: 551–562.
- Lou G, Huang PM. 1988. Hydroxyl-aluminosilicate interlayers in montmorillonite: implications for acidic environments. *Nature* **335**: 625–627.
- McAlister JJ, Smith BJ, Torok A. 2006. Element partitioning and potential mobility within surface dusts on buildings in a polluted urban environment, Budapest. *Atmospheric Environment* **40**: 6780–6790.
- Minitti ME, Weitz CM, Lane MD, Bishop JL. 2007. Morphology, chemistry, and spectral properties of Hawaiian rock coatings and implications for Mars. *Journal of Geophysical Research* **112**: E05015. DOI: 10.1029/2006JE002839
- Nlaist, NioAlSaT. 2005. Atlas of Eh – pH diagrams. Intercomparison of thermodynamic data bases. *Geological Survey of Japan Open File Report* **419**: 1–287.
- Paradise TR. 2005. Petra revisited: an examination of sandstone weathering research in Petra, Jordan. *Geological Society of America Special Paper* **390**: 39–49.
- Perel'man AI. 1966. *Landscape geochemistry*. (Translation No. 676, Geological Survey of Canada, 1972). Vysshaya Shkola: Moscow.
- Perry RS, Lynne YB. 2006. New insights into natural records of planetary surface environments: the role of silica in the formation and diagenesis of desert varnish and siliceous sinter. *Lunar and Planetary Science* **37**: 1292.
- Perry RS, Lynne BY, Sephton MA, Kolb VM, Perry CC, Staley JT. 2006. Baking black opal in the desert sun: the importance of silica in desert varnish. *Geology* **34**: 537–540.
- Perry RS, Sephton MA. 2007. Reply. *Geology* **35**(1): 123. DOI: 10.1130/G23663Y.1
- Peterson J, Moresby J. 1979. Subglacial travertine and associated deposits in the Carstensz area, Irian Jaya, Republic of Indonesia. *Zeitschrift für Gletscherkunde und Glaziologie* **15**: 23–26.
- Robinson DA, Williams RBG. 1987. Surface crusting of sandstones in southern England and northern France. In *International Geomorphology 1986 Part II*, Gardiner V (ed.). John Wiley & Sons: Chichester; 623–635.
- Robinson DA, Williams RBG. 1992. Sandstone weathering in the High Atlas, Morocco. *Zeitschrift für Geomorphologie* **36**: 413–429.
- Schindler M, Fayek M, Hawthorne FC. 2010. Uranium-rich opal from the Nopal I uranium deposit, Pena Blanca, Mexico: evidence for the uptake and retardation of radionuclides. *Geochimica et Cosmochimica Acta* **74**: 187–202.
- Smith BJ. 1988. Weathering of superficial limestone debris in a hot desert environment. *Geomorphology* **1**: 355–367.
- Smith BJ, McAlister JJ, Baptista-Neto JA, Silva MAM. 2007. Post-depositional modification of atmospheric dust on a granite building in central Rio de Janeiro: implications for surface induration and subsequent stone decay. *Geological Society, London, Special Publications* **271**: 153–166.
- Stevenson JJ. 1881. *Report on the US Geographical Surveys West of the One Hundredth Meridian (Wheeler Survey), V. III. Supplement-Geology*. US Army Engineer Department: Washington, DC.
- Tratebas AM, Cerveny N, Dorn RI. 2004. The effects of fire on rock art: microscopic evidence reveals the importance of weathering rinds. *Physical Geography* **25**: 313–333.
- Uchic MD, Holzer L, Inkson BJ, Principe EL, Munroe P. 2007. Three-dimensional microstructural characterization using focused ion beam tomography. *Materials Research Society Bulletin* **32**: 408–416.
- Watchman A. 1985. *Mineralogical Analysis of Silica Skins Covering Rock Art*. Australian National Parks and Wildlife Service: Canberra.
- Watchman A. 1992. Composition, formation and age of some Australian silica skins. *Australian Aboriginal Studies* **1992**(1): 61–66.
- Weed R, Ackert RJ. 1986. Chemical weathering of Beacon Supergroup sandstones and implications for Antarctic glacial chronology. *South Africa Journal Science* **82**: 513–516.
- Weed R, Norton SA. 1991. Siliceous crusts, quartz rinds and biotic weathering of sandstones in the cold desert of Antarctica. In *Diversity of Environmental Biogeochemistry (Developments in Geochemistry, Vol. 6)*, Berthelin J (ed.). Elsevier: Amsterdam; 327–339.
- Wei H, Sparks RSJ, Liu R, Fan Q, Wang Y, Hong H, Zhang H, Chen H, Jiang C, Dong J, Zheng Y, Pan Y. 2003. Three active volcanoes in China and their hazards. *Journal of Asian Earth Sciences* **21**: 515–526.
- Whalley WB, Gellatly AF, Gordon JE, Hansom JD. 1990. Ferromanganese rock varnish in north Norway: a subglacial origin. *Earth Surface Processes and Landforms* **15**: 265–275.
- Wu TW, Qian ZA. 2003. The relation between the Tibetan winter snow and the Asian summer monsoon and rainfall: an observational investigation. *Journal of Climate* **16**: 2038–2051.
- Young R, Young ARM. 1992. *Sandstone Landforms*. Springer-Verlag: Berlin.
- Zhu X, Wang J, Chen J. 1985. Preliminary studies on the 'litholac' soaking on the Gobi rock surface in Gobi Desert. In *Quaternary Geology and Environment of China*, China, QRAo (eds). China Ocean Press: Beijing; 129.
- Zorin ZM, Churayev N, Esipova N, Sergeeva I, Sobolev V, Gasanov E. 1992. Influence of cationic surfactant on the surface charge of silica and on the stability of aqueous wetting films. *Journal of Colloid and Interface Science* **152**: 170–182.